Articles

Interplay of the Intramolecular Water Vibrations and Hydrogen Bond in N-Methylacetamide-Water Complexes: *Ab Initio* Calculation Studies

Joo-Hee Kim and Minhaeng Cho*

Department of Chemistry and Center for Multidimensional Spectroscopy, Division of Chemistry and Molecular Engineering, Korea University, Seoul 136-701, Korea
Received April 14, 2003

The correlation between the water and N-methylacetamide (NMA) intramolecular vibrational frequencies and the hydrogen-bond length in a variety of NMA-H_2O and NMA-D_2O complexes was investigated by carrying out *ab initio* calculations. As the hydrogen-bond length decreases, the frequencies of bending and stretching modes of the hydrogen-bonding water increases and decreases, respectively, and the amide I and II (III) mode frequencies of the NMA decreases and increases, respectively. In this paper, correlation maps among the amide (I, II, and III) modes of NMA and three intramolecular water modes are thus established, which in turn can be used as guidelines for interpreting two-dimensional vibrational spectra of aqueous NMA solutions.

Key Words : Hydrogen bond, Peptide vibration, 2D spectroscopy

Introduction

The amide I infrared band has been extensively studied because its location and shape can provide useful information on secondary structures of polypeptides and proteins.[1-16] In addition to conventional IR absorption and Raman scattering spectroscopies, a variety of multidimensional vibrational spectroscopies involving multiple IR and Raman transitions have been theoretically suggested and experimentally applied to a variety of molecular systems.[17-48] Hochstrasser and coworkers and Hamm and coworkers recently showed that the two-dimensional IR photon echo and pump-probe methods are particularly useful in studying vibrational couplings among different local amide I modes in short polypeptides, and suggested that these IR analogues of multidimensional nuclear magnetic resonance spectroscopy will be of critical use in determining 3D structure and dynamics of polypeptides in solution.[40,41,43-46]

In addition to these current research interests on the amide I mode dynamics of polypeptides, Cho recently proposed that a 2D vibrational spectroscopy can be of use in studying hydrogen-bonding dynamics in aqueous solution.[48] Since the 2D vibrational spectroscopies require at least doubly vibrationally resonant excitations,[26,48] the two external field frequencies, which can be either IR field frequency or the Raman transition frequency depending on the 2D vibrational spectroscopic technique used, ought to be experimentally controlled to be simultaneously resonant both with a particular vibrational transition of the solute and with that of the H-bonding water molecule.[48]

In order to study H-bond dynamics in the time domain, Gale *et al.* used femtosecond IR pump-probe method to directly investigate the dynamics of H-bonds in liquid water.[49,50] Also, Nienhuys *et al.* carried out a similar experiment for HDO : D_2O solution.[51] Noting that the OH stretching mode frequency is sensitively dependent on the H-bond length, as found by Mikenda,[52] they were able to measure solvatochromic shift revealing real time dynamics of the H-bonds in liquid water. Recently, Woutersen *et al.* used an IR pump-probe method to measure the H-bond lifetime in NMA-methanol solution.[53] They measured time-dependent 2D spectra of the amide I mode and estimated the lifetime of each H-bond to be about 12 picoseconds.

Instead of "photographing" the amide I band of the NMA, one can measure time-dependent solvatochromic shift of the intramolecular vibrational modes of waters H-bonded to the solute NMA. An alternative way to study real-time hydrogen-bond dynamics would be to record the time-dependent fully two-color 2D vibrational spectra, where the 2D cross peak between a given water mode, such as OH stretch or bending, and one of the NMA modes, such as amide I, II, or III modes, is measured. Nevertheless, current laser technology does not allow performing such a 2D vibrational spectroscopic measurement yet due to limitations of scanning in the entire IR frequency range. However, in order to provide a guideline for future 2D vibrational spectroscopic investigations of hydrogen-bonding dynamics of polypeptides dissolved in liquid water, we carried out quantum chemical calculation studies to elucidate correlation between the intramolecular vibrational frequencies of water molecule and the H-bond strength in various NMA-H_2O and NMA-D_2O complexes.

*Corresponding author. E-mail: mcho@korea.ac.kr

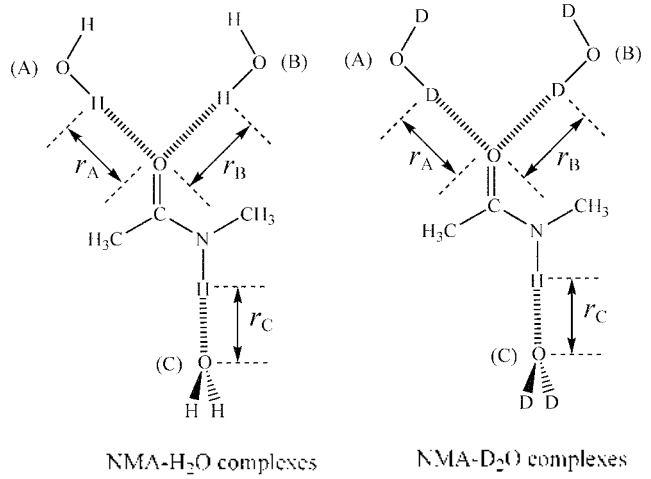

Figure 1. The three hydrogen-bonding sites A, B, and C are depicted in this figure.

Ab Initio Calculation Results for NMA-H_2O and NMA-D_2O Complexes with Varying Intermolecular Distance

Although there already exist a number of literatures on *ab initio* studies of NMA-water complexes,[54-59] most of the previous works concerned about H-bond energies, optimized structures, and amide I mode frequency. Guo and Karplus showed that a single NMA molecule has three H-bonding sites (denoted as A, B, and C) as shown in Figure 1.[54] Using the Gaussian 98 program,[60] we obtained the optimized geometry of NMA-H_2O(A) complex at the RHF/6-311++G** level, where the H-bond distance r_A (see Fig. 1) is found to be 1.9785 Å. Then, the distance r_A is deliberately increased with the relative orientations between the two molecules fixed. For each configuration with the constraint stated above, geometry optimization and vibrational analysis are performed. *Ab initio* calculated vibrational frequencies are scaled by multiplying 0.8929 – although the scaled quantum mechanics, which is to use different scaling factors for each internal coordinate to properly re-scale the normal mode frequencies, has been used, we will invoke a single scaling factor approximation throughout this paper. Similarly, for the other two sites B and C, we carried out the same series of *ab initio* calculations. Also, the same calculations are performed for NMA-D_2O complexes.

When an NMA-H_2O (or NMA-D_2O) complex is formed, the H-bonded H_2O (D_2O) molecule does not belong to the C_{2v} point group any more. However, on the basis of eigenvector element analyses for all the NMA-H_2O and NMA-D_2O complexes, the three water vibrational modes are highly localized in H_2O (D_2O). Therefore, we will still use terms, "bending", "symmetric OH (OD) stretching", and "asymmetric OH (OD) stretching", to refer to the corresponding three normal modes of NMA-H_2O (NMA-D_2O) complex. However, it should be mentioned that, as the number n of surrounding water molecules increases, the normal modes of NMA-$n H_2O$ clusters[59] should be described as collective vibrations of involved water molecules. In the present paper, however, we will focus on the cases of $n = 1$.

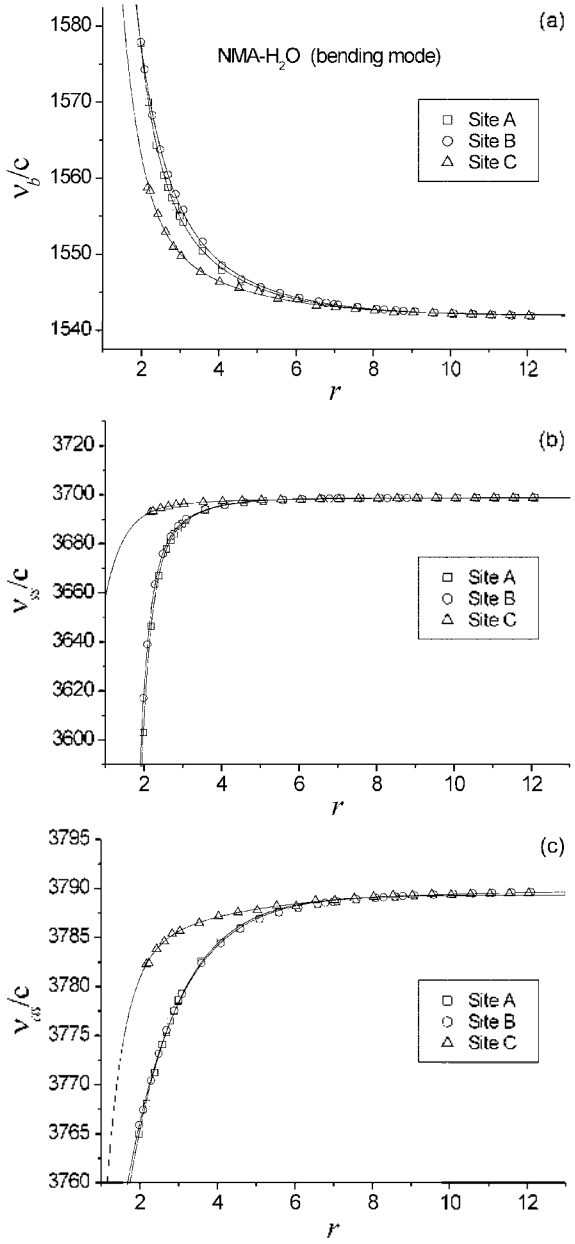

Figure 2. The water bending and two OH stretching mode frequencies are plotted with respect to the hydrogen-bond length, when a single water molecule is attached to one of the three H-bonding sites.

A. Water bending mode in NMA-H_2O and NMA-D_2O. *Ab initio* calculated H_2O and D_2O bending mode frequencies as a function of r_A, r_B, and r_C are plotted in Figure 2(a). As r decreases, the H-bond strength increases and the water bending mode frequency $\tilde{\nu}_b$ increases. Frequency shifts of the water bending mode for the three sites, A, B, and C, are estimated to be 36, 36, and 17 cm^{-1}, respectively, for NMA-H_2O and are 22, 23, and 13 cm^{-1}, respectively, for NMA-D_2O. Note that the bending mode frequency of the water molecule H-bonded to the two sites A or B is strongly blue-shifted in comparison to that to the site C. Typically, the H-bond strength (or energy) of the site C is about two third of

Table 1. Fitting parameters using Eqs. (1), (2), and (3) for the bending mode, symmetric O-H stretching mode, and asymmetric O-H stretching mode frequencies, respectively, for NMA-H_2O (NMA-D_2O) complexes

Mode	Site	η_1	γ_1	η_2	γ_2
Bending	A	18.58	0.542	17.07	2.02
		(12.06)	(0.505)	(9.948)	(1.970)
	B	17.37	0.490	18.51	1.53
		(13.49)	(0.515)	(9.060)	(1.727)
	C	7.930	0.426	3.040	1.99
		(6.709)	(0.4122)	(6.440)	(1.902)
Symmetric Stretching	A	27.96	1.07	67.59	4.07
		(17.09)	(1.031)	(41.92)	(4.273)
	B	27.57	1.100	53.99	4.22
		(16.38)	(1.048)	(34.00)	(4.413)
	C	2.773	0.380	3.084	2.11
		(2.572)	(0.852)	(1.467)	(3.567)
Asymmetric Stretching	A	24.33	0.789	0	–
		(12.23)	(0.547)	(14.74)	(1.994)
	B	23.49	0.746	0	–
		(15.85)	(0.639)	(9.579)	(2.555)
	C	4.906	0.345	2.539	2.16
		(3.263)	(0.461)	(1.462)	(3.683)

that at the site A or B.[58,59] Due to this relatively weak H-bond strength, the perturbation by the NMA onto the water bending mode is comparatively smaller for the site C than those for the sites A and B. The six data sets are very well fitted by the following double exponentially decaying function,

$$\tilde{\nu}_b = \tilde{\nu}_b^0 + \eta_1 \exp\{-\gamma_1(r-r_0)\} + \eta_2 \exp\{-\gamma_2(r-r_0)\}, \quad (1)$$

where the gas-phase value $\tilde{\nu}_b^0$ is found to be 1542 cm^{-1}. The optimum H-bond distances, either C=O...HOH (DOD) or N-H...OH_2 (OD_2), denoted as r_0, are 1.9785, 1.9836, and 2.1682 Å, for the sites A, B, and C, respectively. Fitting results for η_i and γ_i (for i = 1, 2) are summarized in Table 1 for the NMA-H_2O and NMA-D_2O complexes, and fitted curves are shown in Figures 2(a) and 3(a), respectively. In Figure 4(a), the IR intensity, which is a square of the transition dipole moment, of the water bending mode is plotted (the dimension of the IR intensity calculated with the Gaussian 98 is kilometer/mole). The r-dependencies of the bending mode intensities for both NMA-H_2O and NMA-D_2O are almost similar to each other, but the bending mode IR intensity of H_2O is about twice of that of D_2O.

B. Water symmetric stretching mode. The symmetric O-H stretching mode frequencies for the three cases are plotted in Figure 2(b), and are fitted with the following function,

$$\tilde{\nu}_{ss} = \tilde{\nu}_{ss}^0 + \eta_1[1 - \exp\{-\gamma_1(r-r_0)\}] + \eta_2[1 - \exp\{-\gamma_2(r-r_0)\}], \quad (2)$$

where $\tilde{\nu}_{ss}^0$ are found to be 3603.1, 3617.1, and 3692.9 cm^{-1}

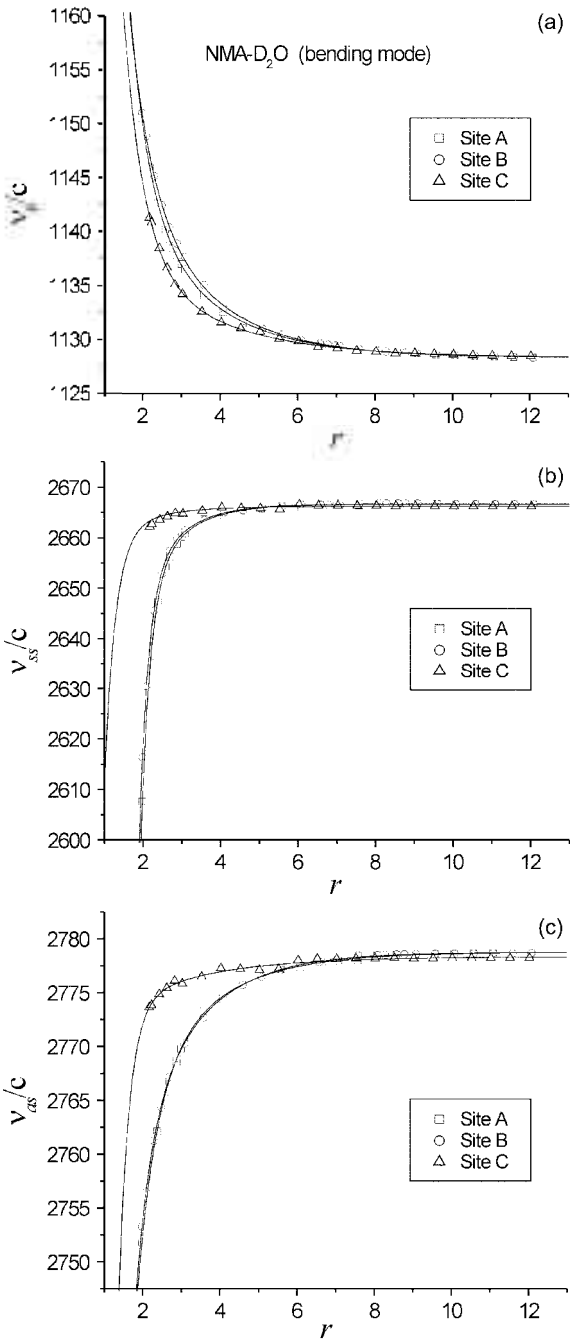

Figure 3. The bending and two OD stretching mode frequencies of NMA-D_2O complexes are plotted with respect to the hydrogen-bond length.

for the sites A, B, and C of NMA-H_2O system, respectively, and are 2607.6, 2616.3, and 2662.2 cm^{-1}, respectively, for the three sites of NMA-D_2O system. Frequency shifts of the symmetric O-H (O-D) stretching mode are 96 (59), 82 (50), and 5.8 (4.0) cm^{-1}, respectively. In contrast to the bending mode, the symmetric stretching mode frequency is strongly red-shifted as the water molecule approaches to the NMA. This means that, as r decreases, effective reduced mass of the stretching mode increases and the O-H bond strength weakens a bit. Also, it is noted that the symmetric O-H stretching mode of the water molecule at the site C is just

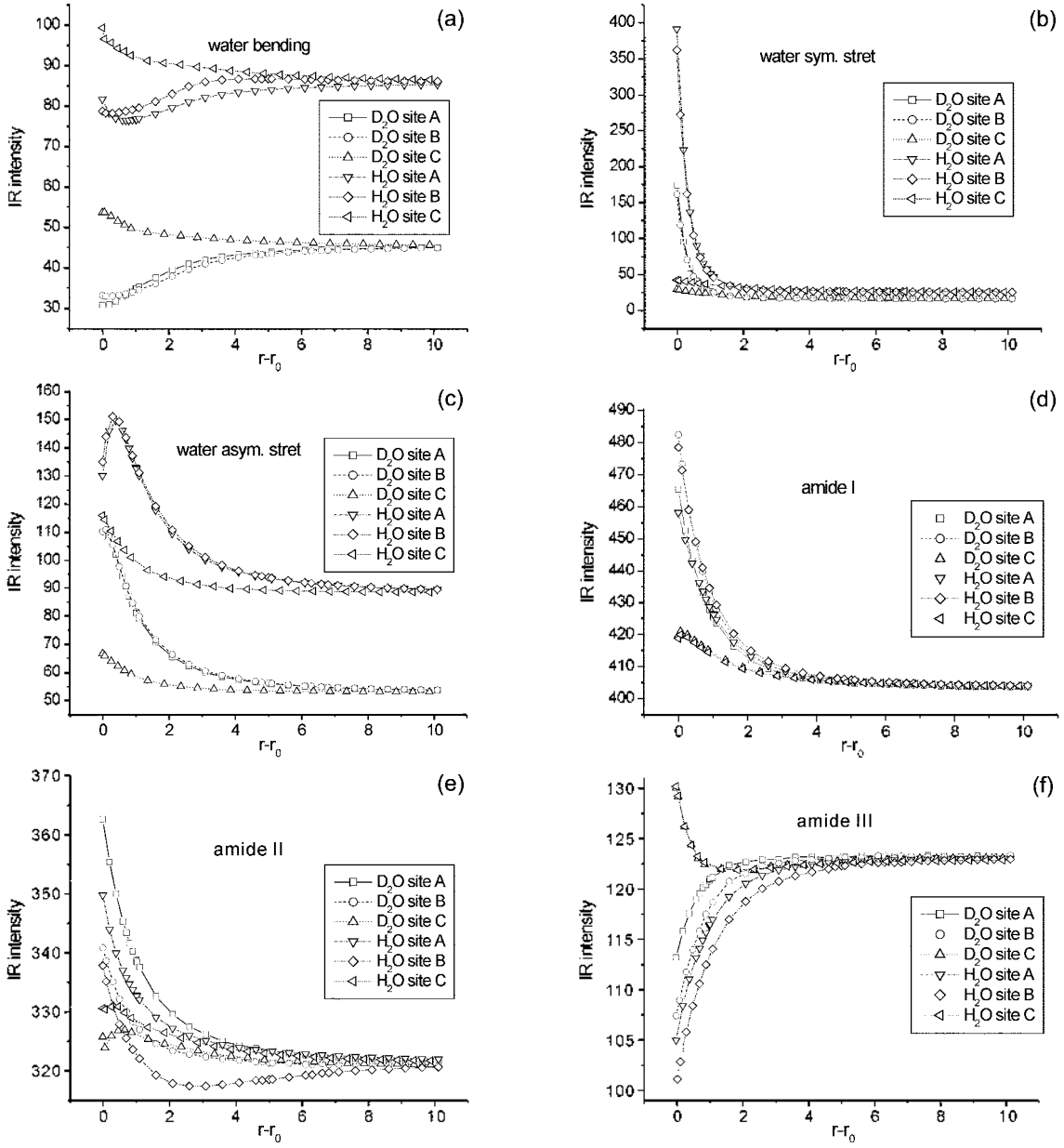

Figure 4. The IR intensities of the water bending, symmetric OH (OD) stretching, and asymmetric OH (OD) stretching, NMA amide I, II, and III modes are plotted with respect to the H-bond length for the six cases of NMA-H_2O and NMA-D_2O complexes.

slightly red-shifted, whereas the symmetric O-H stretch frequency shifts of waters at the sites A and B are notably large even in comparison to other vibrational degrees of freedom. It is also interesting to note that $\tilde{\nu}_{ss}$ of H_2O at the sites A and B is a very quickly varying function of the intermolecular distance. Therefore, the symmetric stretching mode can be a good probe for H-bond dynamics when the two-color IR pump-probe or photon echo methods are employed to investigate the short-time H-bond dynamics of aqueous polypeptide solutions. In Fig.4(b), the IR intensity of the symmetric O-H (O-D) stretching mode is plotted. It is interesting to note that (1) the symmetric O-H(D) stretching mode intensity increases dramatically as the water molecule forms a H-bond to NMA and (2) it is a quickly varying function of r similar to ω_{ss}.

C. Water asymmetric stretching mode. The asymmetric O-H (O-D) stretching mode frequencies for the three cases are plotted in Figure 2(c), (3(c)). The fitting function used is

$$\tilde{\nu}_{as} = \tilde{\nu}_{as}^{0} + \eta_1[1 - \exp\{-\gamma_1(r - r_0)\}] + \eta_2[1 - \exp\{-\gamma_2(r - r_0)\}], \quad (3)$$

where $\tilde{\nu}_{as}^{0}$ values for the three sites A, B, and C of NMA-H_2O (D_2O) are 3765 (2751.8), 3765.9 (2753.3), and 3782.3 (2773.6) cm^{-1}, respectively. Frequency shifts for the three cases are 24.6 (27.0), 23.8 (25.4), and 7.2 (4.7) cm^{-1}, respectively. These values are comparatively smaller than those of symmetric stretching modes. The asymmetric stretching mode is a relatively slowly varying function of the H-bond

distance, in comparison to the symmetric stretching mode. In Figure 4(c), the IR intensity of the asymmetric O-H (O-D) stretching mode is plotted.

D. Amide I mode of NMA in NMA-H_2O and NMA-D_2O. The amide I mode of a peptide bond is an out-of-phase combination of largely C=O stretching and CN stretching. In Ref. [59], we presented a detailed discussion on the hydration effect on the amide I mode frequency. Nevertheless, we didn't attempt to make a fit with the following function,

$$\tilde{\nu}_I = \tilde{\nu}_I^0 + \eta_1(1 - \exp\{-\gamma_1(r - r_0)\}) + \eta_2(1 - \exp\{-\gamma_2(r - r_0)\}), \quad (4)$$

to the r-dependent amide I mode frequency of NMA-H_2O and NMA-D_2O systems (see Fig. 5(a)). Here, $\tilde{\nu}_I^0$ values for the three sites A, B, and C of NMA-H_2O (D_2O) are 1682.1 (1681.4), 1684.5 (1684.2), and 1697.3 (1696.6) cm^{-1}, respectively. Frequency shift magnitudes for the three cases are 25.2 (25.5), 22.8 (22.7), and 10 (10.1) cm^{-1}, respectively. It should be noted that the amide I mode frequency does not change much when H_2O is replaced with D_2O. This relative insensitivity of the NMA normal modes will be shown for other cases below. In Figure 4(d), the IR intensity of the amide I mode is plotted. As the intermolecular distance between NMA and water molecules decreases, the amide I IR intensity increases. As discussed in Ref. [59] in detail, the electrostatic interaction of the NMA with the partial changes of the water molecule induces an electronic structure change of the NMA, which in turn affects to the molecular structure of the NMA. As a H_2O molecule approaches to the carbonyl group to form a H-bond, the electronic structure of the NMA changes more toward the charge-transfer configuration so that the C=O bond length of the NMA increases and at the same time the amide I mode force constant decreases (the two resonance structures are shown below).

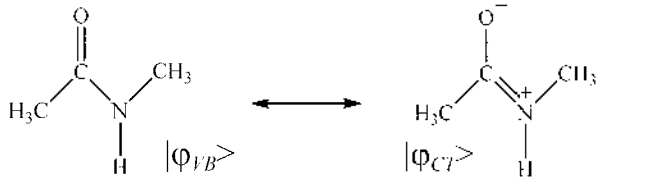

(neutral) valence-bond configuration (zwitterionic) charge-transfer configuration

Denoting δQ_I as the amide I coordinate displacement induced by the electrostatic NMA-water interaction, we found that the transition dipole moment is approximately proportional to the extent of the structural distortion.[61]

$$\left(\frac{\partial \mu_g}{\partial Q_I}\right) \cong \left(\frac{\partial \mu_g}{\partial Q_I}\right)_0^0 + \left[\sum_a \mathbf{r}_a \left(\frac{\partial C_a}{\partial Q_I}\right)_0\right] \delta Q_I \quad (5)$$

Here, $(\partial \mu_g / \partial Q_I)_0^0$ is the transition dipole moment of the gas-phase NMA, and $(\partial C_a / \partial Q_I)_0$ and $\mathbf{r}_a$ are the transition charge and position vector of the NMA a site, respectively.

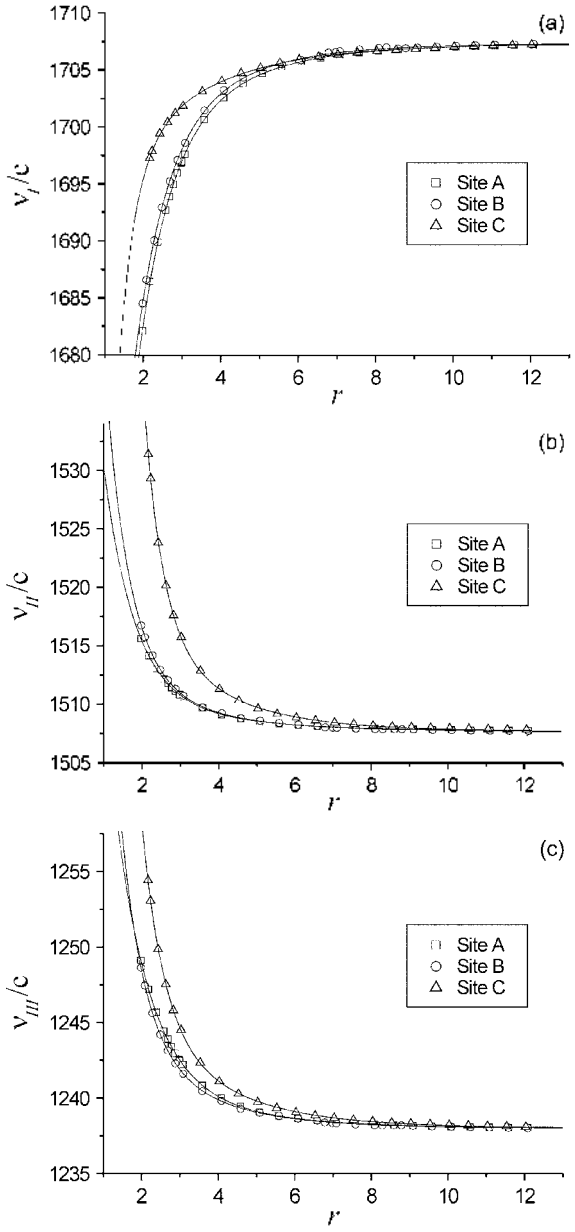

Figure 5. The NMA amide I, II, and III mode frequencies are plotted with respect to the H-bond length for the three cases of NMA-H_2O. Those of NMA-D_2O are quantitatively similar to the cases of NMA-H_2O.

As discussed in Ref. [59], δQ_I can be assumed to be proportional to the C=O bond length displacement, $\delta d_{CO} (\equiv d_{CO} - d_{CO}^0)$, as $\delta Q_I \propto \delta d_{CO}$ so that the transition dipole moment of the NMA-water complex is predicted to be linearly proportional to δd_{CO}. In Figure 6, $|(\partial \mu_g / \partial Q_I)_0|$ (in $(Km/mole)^{1/2}$) is plotted with respect to the ab initio calculated δd_{CO}. Although $|(\partial \mu_g / \partial Q_I)_0|$ values for the three different sites deviate from the linear line, the overall trends are successfully described by the above theoretical model.

E. Amide II mode. The amide II mode of peptide bond, which is an out-of-phase combination of largely NH in-plane bending and CN stretching,[6] has been paid some attention, though the amide I and III modes were found to be strongly

Table 2. Fitting parameters using Eqs.(4), (7), and (8) for the amide I, II, and III mode frequencies of NMA-H_2O (NMA-D_2O) complexes

Mode	Site	η_1	γ_1	η_2	γ_2
Amide I	A	8.374	0.42365	16.83	1.216
		(5.843)	(0.30585)	(19.70)	(1.137)
	B	8.234	0.46215	14.59	1.241
		(5.298)	(0.3455)	(17.40)	(1.072)
	C	7.265	0.43386	2.688	2.382
		(7.50)	(0.44662)	(2.569)	(3.270)
Amide II	A	5.559	1.27578	2.338	0.387
	B	5.348	1.63839	3.689	0.487
	C	15.35	2.07248	8.327	0.504
Amide III	A	8.219	1.13509	2.891	0.405
	B	6.089	1.64296	4.529	0.497
	C	9.919	1.77644	6.411	0.462

dependent on secondary structures of polypeptides. For those NMA-H_2O (A, B, or C) complexes with varying r, the amide II mode frequencies are calculated and summarized in Figure 5(b). The fitting function used in this case is

$$\tilde{\nu}_{II} = \tilde{\nu}_{II}^{0} + \eta_1 \exp\{-\gamma_1(r-r_0)\} + \eta_2 \exp\{-\gamma_2(r-r_0)\}, \quad (7)$$

where $\tilde{\nu}_{II}^{0}$ is found to be 1507.7 cm^{-1}. The amplitudes and decay constants of the two exponential components are summarized in Table 2. Unlike the case of amide I mode, the hydrogen-bond of a water molecule to the site C induces comparatively large frequency shift of the amide II mode frequency. This can be understood by noting that the amide II vibration involves largely NH in-plane bending so that the hydrogen-bonded water molecule to the site C greatly perturbs the NH in-plane bending vibration. Frequency shift magnitude is about 24 cm^{-1}. Although not presented in this paper, the deuterium isotope effect on the amide II mode frequency of NMA-D_2O is very small. In Figure 4(e), the IR intensity of the amide II mode is plotted.

F. Amide III mode. The amide III mode is an in-phase combination of NH in-plane bending and CN stretching vibrations.[6] The fitting function used is

$$\tilde{\nu}_{III} = \tilde{\nu}_{III}^{0} + \eta_1 \exp\{-\gamma_1(r-r_0)\} + \eta_2 \exp\{-\gamma_2(r-r_0)\}, \quad (8)$$

where $\tilde{\nu}_{III}^{0}$ is found to be 1238 cm^{-1}. The fitting results are summarized in Table 2 and Figure 5(c). Note that, in comparison to the amide II mode, the frequency of the amide III mode does not change much as a single water molecule makes a H-bond to one of the three sites. The deuterium isotope effect on amide II mode frequency of NMA-D_2O is also found to be very small. In Figure 4(f), the amide III mode intensity is plotted.

G. Correlation between water mode frequencies and NMA amide I mode frequency. Because of the electrostatic field perturbation by the solvated water molecules, the electronic and molecular structures of the NMA change,

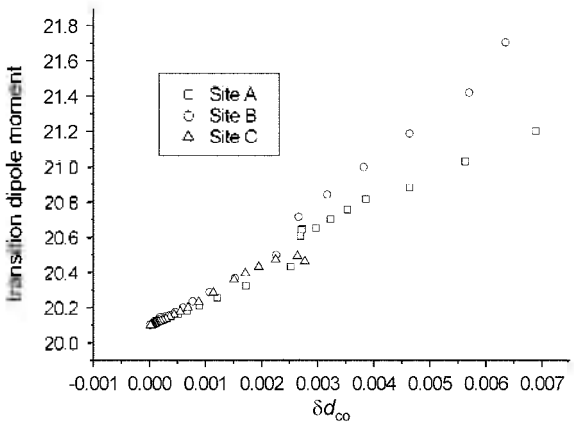

Figure 6. The amide I IR transition dipole moment of NMA-H_2O (A, B, and C) are plotted with respect to δd_{CO} (in Å).

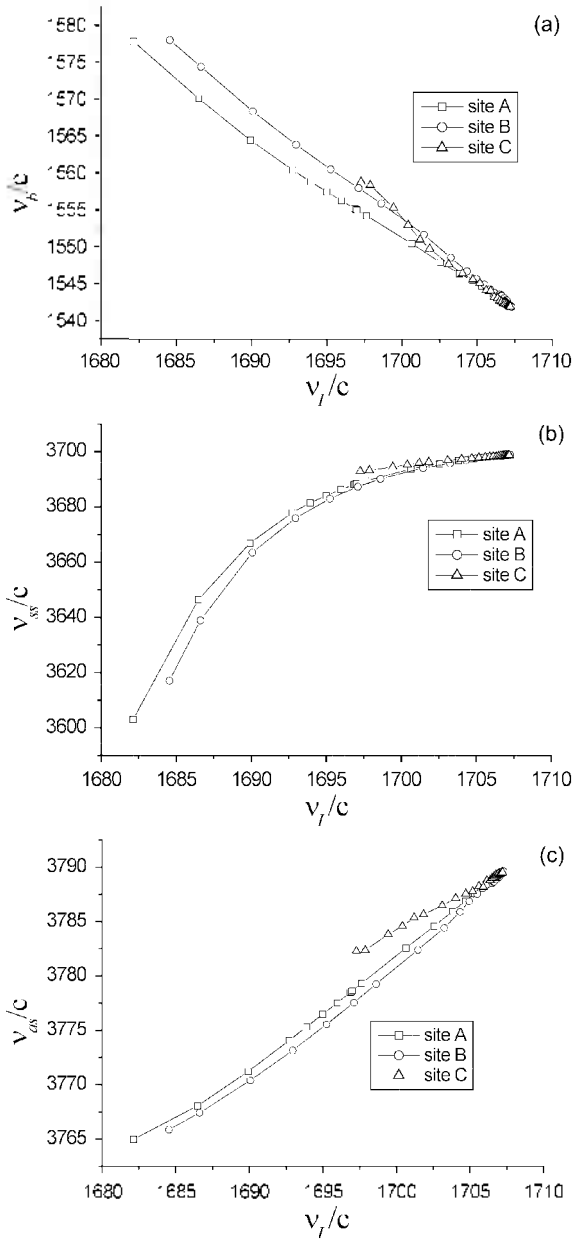

Figure 7. The three water mode frequencies vs. amide I mode frequency.

which in turn modifies the potential energy surfaces of various peptide vibrational modes. Now, from the standpoint of the water molecule in the NMA-H_2O system, NMA is the solvent molecule perturbing the electronic and molecular structures of the water. Therefore, one can infer that there should be a strong correlation between the NMA modes and water modes. In Figures 7, the bending and two stretching mode frequencies are plotted with respect to the amide I mode frequency. The frequency of the water bending mode, which was found to be strongly coupled to the amide I mode because of the small frequency difference between the two, is observed to be almost linearly proportional to that of the amide I mode. On the other hand, the symmetric and asymmetric stretching mode frequencies are nonlinearly correlated with the amide I mode frequency.

Two-Dimensional Vibrational Spectroscopic Implications

Two-dimensional vibrational spectroscopy, such as IR-IR-Vis FWM,[24,26,33,48,62] involves doubly vibrationally resonant processes. Let's consider the IR-IR-Vis sum-frequency-generation (IIV-SFG) process.[33] In the frequency domain, the corresponding third-order susceptibility can be approximately written as, in the doubly vibrationally resonant limit,

$$\chi(\omega_1, \omega_2, \omega_3) \propto \frac{A_{jk}(\mathbf{R}_{pep}, \mathbf{R}_{wat})}{\{\omega_1 - \omega_j^{pep} + i\Gamma_j\}\{\omega_1 + \omega_2 - \omega_j^{pep} - \omega_k^{wat} + i\Gamma_{ni}\}} \quad (9)$$

where the first two IR and visible field frequencies are denoted as ω_1, ω_2, and ω_3, respectively. $\omega_j^{pep}(\mathbf{R}_{pep}, \mathbf{R}_{wat})$ (for $j = I, II, III$, etc) and $\omega_k^{wat}(\mathbf{R}_{pep}, \mathbf{R}_{wat})$ (for $k = b, ss, as$) are the jth and kth mode frequencies of NMA and water, respectively. $\mathbf{R}_{pep}$ and $\mathbf{R}_{wat}$ are coordinates specifying the orientations and locations of the peptide and water molecules, respectively. Γ_j and Γ_k are vibrational dephasing constants. The phase-matched IIV-SFG field frequency is $\omega_1 + \omega_2 + \omega_3$. The proportionality constant $A_{jk}(\mathbf{R}_{pep}, \mathbf{R}_{wat})$ determining the corresponding cross peak intensity is given by a product of transition dipole and transition polarizability matrix elements and is also determined by the magnitudes of electric and mechanical anharmonicities of the peptide-water complex.[33] Noting that only those water molecules strongly interacting with the peptide can have nonzero vibrational coupling, *i.e.*, $A_{jk}(\mathbf{R}_{pep}, \mathbf{R}_{wat}) \neq 0$, the above two-dimensional vibrational spectroscopic method can be used to selectively study the H-bond effects on the intermolecular vibrational interaction between NMA and water molecules. Since, in the present paper, the correlation between amide mode frequencies and water mode frequencies was elucidated, the location of the cross peak and the intermolecular-distance-dependent amplitude, $A_{jk}(\mathbf{R}_{pep}, \mathbf{R}_{wat})$,[30] could provide direct information on the hydrogen-bond structure of water molecules around the peptide.

Another type of 2D vibrational spectroscopy that has been used widely is a two-color IR pump-probe.[49-51] Tuning the pump field frequency to be resonant with one of the amide mode transitions as well as controlling the probe field frequency being resonant with one of the three water mode transitions, one can measure time-dependent evolution of the H-bond dynamics by using the relationships discussed in this paper. In this regard, the symmetric OH stretching mode of water molecules H-bonded to the NMA sites A and B can be the primary target for this type of experiment measuring equilibrium and/or non-equilibrium H-bond structures, because ω_{ss} and its IR intensity were found to be a quickly varying function of the intermolecular distance.

Summary

We presented *ab initio* calculation results on the interplay of water and NMA intramolecular vibrational properties and H-bond strength. The frequencies of bending, symmetric stretching, and asymmetric stretching modes of H-bonded water molecules were investigated and were found to be sensitively dependent on the hydrogen-bond strength. Also, the amide I, II, and III mode frequencies of NMA-H_2O and NMA-D_2O complexes were calculated as a function of the intermolecular distance between the NMA and H_2O (D_2O). Particularly, the symmetric OH stretching mode was observed to be the most sensitive probe for the H-bond structure. The correlation between the NMA amide I mode frequency and water mode frequencies was established, which in turn can be used to measure hydrogen-bond structure of peptides in aqueous solution by employing a variety of 2-D vibrational spectroscopies.

Acknowledgement. This work was supported by the Creative Research Initiatives Program of KISTEP (MOST, Korea).

References

1. *Spectroscopic Methods for Determining Protein Structure in Solution*; Havel, H. A., Ed.; VCH: New York, U. S. A., 1996.
2. Arrondo, J. L. R.; Goni, F. M. *Progr. Biophys. Mol. Biol.* **1999**, *72*, 367.
3. *Infrared and Raman Spectroscopy of Biological Materials*; Gremlich, H.-U.; Yan, B., Eds.; Marcel Dekker: New York, 2000.
4. Surewicz, W. K.; Mantsch, H. H. *Biochim. Biophys. Acta* **1988**, *952*, 115.
5. Torii, H.; Tasumi, M. In *Infrared Spectroscopy of Biomolecules*; Mantsch, H. H.; Chapman, D., Eds.; Wiley-Liss: New York, U. S. A., 1996; p 1.
6. Krimm, S.; Bandekar, J. *Adv. Protein Chem.* **1986**, *38*, 181.
7. Susi, H.; Byler, D. M. *Biochem. Biophys. Res. Commun.* **1983**, *115*, 391.
8. Prestrelski, S. J.; Byler, D. M.; Thompson, M. P. *Int. J. Pept. Protein Res.* **1991**, *37*, 508.
9. Torii, H.; Tasumi, M. *J. Chem. Phys.* **1992**, *96*, 3379.
10. Choi, J.-H.; Ham, S.; Cho, M. *J. Chem. Phys.* **2002**, *117*, 6821.
11. Cha, S.; Ham, S.; Cho, M. *J. Chem. Phys.* **2002**, *117*, 740.
12. Chen, X. G.; Schweitzer-Stenner, R.; Krimm, S.; Mirkin, N. G.; Asher, S. A. *J. Am. Chem. Soc.* **1994**, *166*, 11141.
13. Chen, X. G.; Asher, S. A.; Schweitzer-Stenner, R.; Mirkin, N. G.; Krimm, S. *J. Am. Chem. Soc.* **1995**, *117*, 2884.
14. Lee, S.-H.; Krimm, S. *Chem. Phys.* **1998**, *230*, 277.

15. Kubelka, J.; Keiderling, T. A. *J. Am. Chem. Soc.* **2001**, *123*, 6142.
16. Kubelka, J.; Keiderling, T. A. *J. Phys. Chem. A* **2001**, *105*, 10922.
17. *Ultrafast Infrared and Raman Spectroscopy*; Fayer, M. D., Ed.; Marcel Dekker: New York, U. S. A., 2001.
18. *Chemical Physics*, **266**, issues 2-3, 2001.
19. Tanimura, Y.; Mukamel, S. *J. Chem. Phys.* **1993**, *99*, 9496.
20. Tominaga, K.; Yoshihara, K. *Phys. Rev. Lett.* **1996**, *74*, 3061.
21. Okumura, K.; Tanimura, Y. *J. Chem. Phys.* **1997**, *106*, 1687; **1997**, *107*, 2267.
22. Cho, M.; Okumura, K.; Tanimura, Y. *J. Chem. Phys.* **1997**, *108*, 1326.
23. Tokmakoff, A.; Lang, M. J.; Larsen, D. S.; Fleming, G. R.; Chernyak, V.; Mukamel, S. *Phys. Rev. Lett.* **1997**, *79*, 2702.
24. Zhao, W.; Chernyak, V.; Mukamel, S. *J. Chem. Phys.* **1998**, *110*, 5011.
25. Steffen, T.; Duppen, K. *Chem. Phys. Lett.* **1997**, *273*, 47.
26. Cho, M. In *Advances in Multi-photon Process and Spectroscopy*; Lin, S. H.; Villaeys, A. A.; Fujimura, Y., Eds.; World Scientific: Singapore, 1999; Vol. 12, p 229.
27. Hahn, S.; Park, K.; Cho, M. *J. Chem. Phys.* **1999**, *111*, 4121.
28. Park, K.; Hahn, S.; Cho, M. *J. Chem. Phys.* **1999**, *111*, 4131.
29. Cho, M. *J. Chem. Phys.* **1999**, *111*, 4140.
30. Hahn, S.; Kwak, K.; Cho, M. *J. Chem. Phys.* **1999**, *112*, 4553.
31. Cho, M. *J. Chem. Phys.* **2000**, *112*, 9978.
32. Kaufman, L. J.; Heo, J.; Fleming, G. R.; Sung, J.; Cho, M. *Chem. Phys.* **2001**, *266*, 251.
33. Cho, M. *Phys. Rev. A* **2000**, *61*, 23406.
34. Blank, D.; Kaufman, L.; Fleming, G. R. *J. Chem. Phys.* **2000**, *113*, 771.
35. Zhao, W.; Wright, J. C. *Phys. Rev. Lett.* **1999**, *83*, 1950.
36. Bonn, M.; Hess, Ch.; Miners, J. H.; Bakker, H. J.; Heinz, T. F.; Cho, M. *Phys. Rev. Lett.* **2001**, *86*, 1566.
37. Sung, J.; Cho, M. *J. Chem. Phys.* **2000**, *113*, 7072.
38. Sung, J.; Silbey, R. J.; Cho, M. *J. Chem. Phys.* **2001**, *115*, 1422.
39. Okumura, K.; Jonas, D. M.; Tanimura, Y. *Chem. Phys.* **2001**, *266*, 237.
40. Hamm, P.; Lim, M.; Hochstrasser, R. M. *J. Phys. Chem. B* **1998**, *102*, 6123.
41. Hamm, P.; Lim, M.; DeGrado, W. F.; Hochstrasser, R. M. *J. Phys. Chem. A* **1999**, *103*, 10049.
42. Piryatinski, A.; Chernyak, V.; Mukamel, S. *In Ultrafast Infrared and Raman Spectroscopy*; Fayer, M. D., Ed.; Marcel Dekker: New York, U. S. A., 2001; p 349.
43. Woutersen, S.; Hamm, P. *J. Phys. Chem. B* **2000**, *104*, 11316.
44. Hamm, P.; Lim, M.; DeGrado, W. F.; Hochstrasser, R. M. *Proc. Natl. Acad. Sci.* **1999**, *96*, 2036.
45. Hamm, P.; Lim, M.; Hochstrasser, R. M. *J. Phys. Chem. B* **1998**, *102*, 6123.
46. Woutersen, S.; Hamm, P. *J. Phys. Chem. B* **2000**, *104*, 11316.
47. Scheurer, C.; Piryatinski, A.; Mukamel, S. *J. Am. Chem. Soc.* **2001**, *123*, 3114.
48. Cho, M. *PhysChemComm.* **2002**, *5*, 40.
49. Gale, G. M.; Gallot, G.; Hache, F.; Lascoux, N.; Bratos, S.; Leicknam, J.-Cl. *Phys. Rev. Lett.* **1999**, *82*, 1068.
50. Bratos, S.; Gale, G. M.; Gallot, G.; Hache, F.; Lascoux, N.; Leicknam, J.-Cl. *Phys. Rev. E* **2000**, *61*, 5211.
51. Nienhuys, H.-K.; Woutersen, S.; van Santen, R. A.; Bakker, H. J. *J. Chem. Phys.* **1999**, *111*, 1494.
52. Mikenda, W. *J. Mol. Struct.* **1986**, *147*, 1.
53. Woutersen, S.; Mu, Y.; Stock, G.; Hamm, P. *Chem. Phys.* **2001**, *266*, 137.
54. Guo, H.; Karplus, M. *J. Phys. Chem.* **1992**, *96*, 7273.
55. Guo, H.; Karplus, M. *J. Phys. Chem.* **1994**, *98*, 7104.
56. Dixon, D. A.; Dobbs, K. D.; Valentini, J. J. *J. Phys. Chem.* **1994**, *98*, 13435.
57. Han, W.-G.; Suhai, S. *J. Phys. Chem.* **1996**, *100*, 3942.
58. Torii, H.; Tatsumi, T.; Tasumi, M. *J. Raman Spectrosc.* **1998**, *29*, 537.
59. Ham, S.; Kim, J.-H.; Lee, H.; Cho, M. *J. Chem. Phys.* **2003**, *118*, 3491.
60. Frisch, M. J.; Trucks, G. W.; Schlegel, H. B.; Scuseria, G. E.; Robb, M. A.; Cheeseman, J. R.; Zakrzewski, V. G.; Montgomery, J. A.; Stratmann, Jr., R. E.; Burant, J. C.; Dapprich, S.; Millam, J. M.; Daniels, A. D.; Kudin, K. N.; Strain, M. C.; Farkas, O.; Tomasi, J.; Barone, V.; Cossi, M.; Cammi, R.; Mennucci, B.; Pomelli, C.; Adamo, C.; Clifford, S.; Ochterski, J.; Petersson, G. A.; Ayala, P. Y.; Cui, Q.; Morokuma, K.; Malick, D. K.; Rabuck, A. D.; Raghavachari, K.; Foresman, J. B.; Cioslowski, J.; Ortiz, J. V.; Baboul, A. G.; Stefanov, B. B.; Liu, G.; Liashenko, A.; Piskorz, P.; Komaromi, I.; Gomperts, R.; Martin, R. L.; Fox, D. J.; Keith, T.; Al-Laham, M. A.; Peng, C. Y.; Nanayakkara, A.; Gonzalez, C.; Challacombe, M.; Gill, P. M. W.; Johnson, B.; Chen, W.; Wong, M. W.; Andres, J. L.; Gonzalez, C.; Head-Gordon, M.; Replogle, E. S.; Pople, J. A. *Gaussian 98, Revision A.7*; Gaussian, Inc.: Pittsburgh, PA, 1998.
61. Cho, M. *J. Chem. Phys.* **2003**, *118*, 3480.
62. Park, K.; Cho, M. *J. Chem. Phys.* **1998**, *109*, 10559.